


# Photoexcitation Cascade and Quantum-Relativistic Jets in Graphene

Cyprian Lewandowski and L. S. Levitov

*Department of Physics, Massachusetts Institute of Technology, Cambridge, Massachusetts 02139, USA*

 (Received 6 June 2017; published 14 February 2018)

In Dirac materials linear band dispersion blocks momentum-conserving interband transitions, creating a bottleneck for electron-hole pair production and carrier multiplication in the photoexcitation cascade. Here we show that the decays are unblocked and the bottleneck is relieved by subtle many-body effects involving multiple off-shell  $e$ - $h$  pairs. The decays result from a collective behavior due to simultaneous emission of many soft pairs. We discuss characteristic signatures of the off-shell pathways, in particular the sharp angular distribution of secondary carriers, resembling relativistic jets in high-energy physics. The jets can be directly probed using solid-state equivalent of particle detectors. Collinear scattering enhances carrier multiplication, allowing for emission of as many as  $\sim 10$  secondary carriers per single absorbed photon.

DOI: 10.1103/PhysRevLett.120.076601

The general question of how an excited electron partitions its energy among lower-energy excitations is central to our understanding of carrier dynamics in solids. One key pathway is the emission of particle-hole pairs, a process that leads to carrier multiplication in a photoexcitation cascade. Physics becomes particularly interesting in Dirac materials with linear carrier dispersion [1], where strong interactions enhance the carrier-carrier scattering whereas momentum conservation greatly restricts the phase space available for such processes and (naively) may entirely block decays [see Fig. 1(a)] [2–4].

In models of photoresponse it is usually taken for granted that energy is conserved at all times and throughout all stages of the cascade, with transitions taking place “on shell” [5–10]. Here we introduce the off-shell processes involving virtual states that disobey the energy-momentum relation. We argue that these processes dominate photoresponse, producing large numbers of secondary electron-hole ( $e$ - $h$ ) pairs. These processes are conceptually similar to the off-shell processes in high-energy physics responsible for the formation of relativistic jets.

The dilemma faced by a photoexcited electron in a Dirac material can be summarized through the quantum-mechanical uncertainty relation. The latter permits energy nonconservation for relatively short time intervals not exceeding the inverse decay time,

$$\Delta\varepsilon \lesssim \frac{\hbar}{\tau}. \quad (1)$$

Suppose the dependence  $\tau$  vs  $\Delta\varepsilon$  is such that increasing the “offshellness”  $\Delta\varepsilon$  opens up a large phase space for decays. In this case, the off-shell processes with large  $\Delta\varepsilon$  will win over the processes with a smaller  $\Delta\varepsilon$ .

As we will see, the offshell dynamics has striking consequences for the photoexcitation cascade and, ultimately, the photoresponse. First, it allows a primary

photoexcited  $e$ - $h$  pair to generate multiple secondary pairs, produced through the processes of the type pictured in Fig. 1(b). These pairs are typically considerably softer than the primary pair, forming a broadband energy distribution

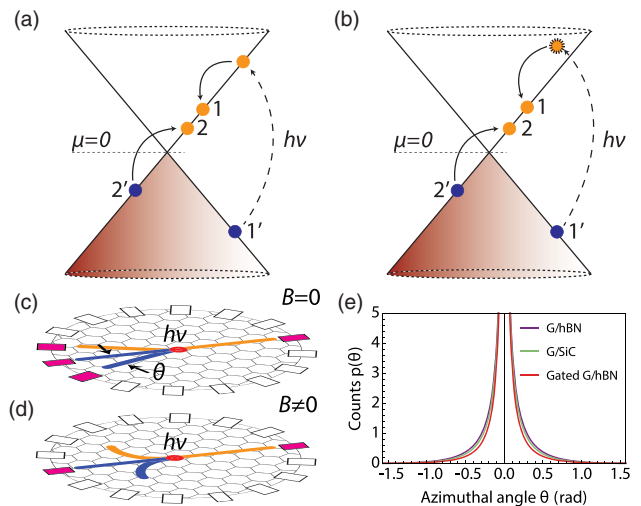


FIG. 1. (a),(b) Types of carrier scattering in a Dirac band. The on-shell processes (a) are subject to energy and momentum conservation, and, therefore, cannot trigger transitions between physical states in different linearly dispersing bands [8,11]. This bottleneck is relieved by the off-shell processes (b) mediated by virtual states residing off the Dirac cone. This triggers collinear scattering and emission of multiple soft  $e$ - $h$  pairs with a tightly focused jetlike angular distribution. The jets can be probed as illustrated in (c),(d). A photon (red dot) creates an  $e$ - $h$  jet that is detected by a group of adjacent contacts (activated contacts are shown in magenta). A weak  $B$  field blocks soft pairs from reaching contacts (d), allowing for the energy distribution to be directly probed. (e) Angular distribution of soft pairs in the jets. The  $e$ - $e$  interaction screened by the substrate and gate is described in [12].

analyzed below. Second, due to the collinear character of relevant electron-electron ( $e$ - $e$ ) collision processes, the secondary pairs are preferentially emitted along the primary pair velocity direction, forming a jetlike angular distribution [see Figs. 1(c), 1(e)]. The latter can be studied experimentally using a solid-state analog of a particle detector realized as a circular array of photocurrent detectors [13–15], see Fig. 1(c).

Energy-resolved studies of soft pairs can be performed using an external magnetic field that deflects the orbits of soft carriers but has little effect on the more energetic carriers [see Fig. 1(d)]. A field of strength  $B$  prevents carriers with energies below the threshold  $\varepsilon < eBvR/2$  from reaching the detectors at a distance  $R$ , providing a direct probe of the energy distribution of soft pairs.

Our system is described by the Hamiltonian for  $N$  species of massless Dirac particles ( $N = 4$  for graphene):

$$\mathcal{H} = \sum_{i=1\dots N} \sum_{\mathbf{k}} \psi_{\mathbf{k},i}^\dagger (\hbar v \boldsymbol{\sigma} \cdot \mathbf{k}) \psi_{\mathbf{k},i} + \mathcal{H}_{e-e}. \quad (2)$$

Here the optical field is included through minimal coupling  $\mathbf{k} \rightarrow \mathbf{k} - (e/\hbar c)\mathbf{A}$  and  $\mathcal{H}_{e-e}$  describes  $e$ - $e$  interactions [12]. We focus on the processes in a pristine material (undoped and disorder-free), assuming high mobility, long mean free paths and, for simplicity, ignoring the effects of electron-phonon scattering. While in real materials these effects may be significant, reducing the net response, they do not alter the outcome of competition between the on-shell and off-shell  $e$ - $e$  processes.

There are several ways to develop perturbation theory for  $e$ - $e$  scattering: the weak-coupling approach uses small fine structure constant  $\alpha = (e^2/\kappa\hbar v) \ll 1$ , the large- $N$  approach uses as a small dimensionless coupling  $1/N \ll 1$  with an RPA-screened interaction [16–19]. The latter approach (which we use below) is, in principle, capable of dealing with systems at strong coupling  $\alpha > 1$  as long as the number of species  $N$  is large enough. The resulting diagrammatics resembles that of QED, modulo replacing photon propagator by the dynamically screened Coulomb interaction [16].

A salient feature of Feynman diagrams describing the processes of secondary pair creation (see Fig. 2) is the double-log divergences similar to those familiar in QED and

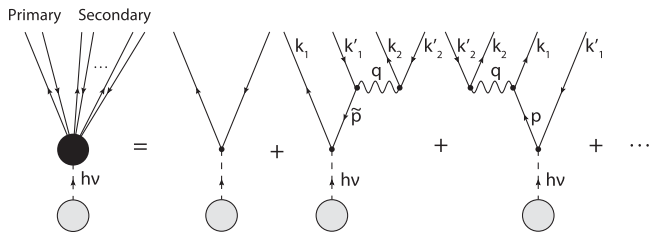


FIG. 2. Diagrammatic representation of single-photon absorption. Dashed lines describe interaction with a photon source, straight lines with arrows denote electron and hole propagators, wavy lines denote the dynamically screened Coulomb interaction, Eq. (3).

QCD [20–22]. Below we analyze excitation of  $e$ - $h$  pairs described by  $\log^2$ -divergent diagrams, which reflect production of infinitely many soft  $e$ - $h$  pairs. We show that in the large- $N$  framework the rate for producing  $p$  pairs behaves as  $N^{-p} \log^{2p}$ . Multiple  $\log^2$  divergences can be tackled by resumming the contributions with the highest powers of  $\log^2$  [22], or by more refined approaches [20,21]. This approach allows us to obtain a detailed picture of the cascade, including the angular distribution and energy spectrum of secondary pairs. We stress that the behavior of log divergences in graphene field theory is close to that in  $(3+1)$ -dimensional QED [16], whereas the behavior in  $(2+1)$ -dimensional QED is quite different [23,24] but is not directly relevant here.

We note that in a realistic setting the linear dispersion of Dirac bands, which is crucial for our analysis, is an asymptotic behavior valid at low enough energies. This makes the properties of soft pairs universal and largely insensitive to the details of band dispersion. For example, the trigonal warping of Dirac cones is significant at high energies but vanishes near the Dirac point [1]. Another, potentially more critical, deformation of the Dirac cones arises due to interaction-induced velocity renormalization. The latter leads to dispersion “steepening” close to the Dirac point. This has two effects: one is further suppression of the on-shell relaxation rate, the other is a decrease in the phase space available for particles with small offshellness. However, since these effects occur at a first-log order, they are subleading to the  $\log^2$  effects analyzed below.

Photon absorption is represented diagrammatically as a sum of contributions with one incoming photon leg and many outgoing particle legs, with the screened  $e$ - $e$  interaction replacing photon propagator in the corresponding QED diagrams. The lowest order tree-level diagrams are shown in Fig. 2. The diagram with two particle legs describes creation of a primary  $e$ - $h$  pair, an on-shell process with no virtual states. Such virtual states, present in the diagrams of higher order, are described by internal fermion lines without open ends. These states reside off shell, as indicated in Eq. (1). The higher-order diagrams describe creation of multiple secondary pairs, with summation over virtual states generating double-log divergences as discussed below. The wavy lines in Fig. 2 represent the dynamically screened interaction expressed through an exact polarization function as

$$\tilde{V}_{q,\omega} = \frac{V_q}{1 - V_q \Pi(\mathbf{q}, \omega)}, \quad V_q = \frac{2\pi e^2}{\kappa |q|}, \quad (3)$$

with  $\mathbf{q}$  and  $\omega$  denoting the transferred momentum and frequency, and  $\kappa$  is the dielectric constant. The values of  $\kappa$  for different substrates are discussed in [12] along with the model used to generate Fig. 1 and a modification of  $V_q$  describing screening by the gate. Divergence in the polarization function  $\Pi(\mathbf{q}, \omega)$  softens the small- $q$  divergence of  $V_q$ . We use a simple expression [11,25],

$$\Pi(\mathbf{q}, \omega) = -\frac{iN\mathbf{q}^2}{16\hbar} \frac{1}{\sqrt{\omega^2 - v^2\mathbf{q}^2}}, \quad (4)$$

describing the interband  $e$ - $h$  pair excitations,  $\omega > vq$ .

Crucially, even a single secondary pair creation is a strongly off-shell process. Indeed, linearity of band dispersion  $\varepsilon(\mathbf{k})$  renders the  $e$ - $e$  scattering processes obeying energy and momentum conservation to be of a strictly collinear character [2]. However, collinear scattering is subject to a phase space constraint that makes the transition rate vanish [see Fig. 1(a)] [11]. In contrast, no phase space constraints arise for the off-shell processes [see Fig. 1(b)], and, in fact, the large phase space generates the double log-divergent contributions to the transition rate. This behavior extends to all higher-order multiple pair creation processes.

Turning to the quantitative analysis, we consider the second and third diagrams pictured in Fig. 2, which describe an initial photoexcited  $e$ - $h$  pair with energy and momentum positioned off-shell that excites a secondary  $e$ - $h$  pair via an interband transition. At the end, all participating particles are found in the on-shell states at the Dirac cone. The transition rate for this process, within the standard golden rule approach, takes the form

$$W_{0 \rightarrow 1} = \frac{2\pi}{\hbar} N^2 \sum_{\mathbf{k}'_1 + \mathbf{k}'_2 = \mathbf{k}_1 + \mathbf{k}_2} f_{\mathbf{k}'_1}(1 - f_{\mathbf{k}_1}) f_{\mathbf{k}'_2}(1 - f_{\mathbf{k}_2}) |\mathcal{A}|^2 \delta_\varepsilon. \quad (5)$$

Here  $f_{\mathbf{k}}$  is the Fermi function,  $h\nu$  is the absorbed photon energy (we set photon momentum equal zero), and  $\delta_\varepsilon = \delta(\varepsilon_{\mathbf{k}_1} + \varepsilon_{\mathbf{k}_2} - \varepsilon_{\mathbf{k}'_1} - \varepsilon_{\mathbf{k}'_2} - h\nu)$ . The transition matrix element  $\mathcal{A}$  is given by a sum of two second-order contributions, which differ by the order of the operators describing photon absorption and secondary pair creation

$$\mathcal{A} = \langle 1, 2 | M_{\mathbf{q}, \omega} G(\varepsilon_{\mathbf{p}}, \mathbf{p}) \sigma \mathbf{A} + \sigma \mathbf{A} G(\varepsilon_{\tilde{\mathbf{p}}}, \tilde{\mathbf{p}}) M_{\mathbf{q}, \omega} | 1', 2' \rangle, \quad (6)$$

$$|M_{\mathbf{q}, \omega}|^2 = |\tilde{V}_{\mathbf{q}, \omega}|^2 \tilde{F}_{\mathbf{k}_2, \mathbf{k}'_2} F_{\mathbf{k}_1, \mathbf{k}'_1},$$

where  $G(\varepsilon, \mathbf{k})$  is the noninteracting fermion propagator, and we introduced a shorthand notation  $|1, 2\rangle = |\mathbf{k}_1, \mathbf{k}_2\rangle$ ,  $|1', 2'\rangle = |\mathbf{k}'_1, \mathbf{k}'_2\rangle$ , using unprimed and primed symbols for the states of electrons and holes (see Fig. 2). For brevity, we suppress the Dirac spinor structure and incorporate the factor  $ve/c$  in the definition of the optical field  $\mathbf{A}$  (to be restored below). The quantities  $F_{\mathbf{k}, \mathbf{k}'}$  and  $\tilde{F}_{\mathbf{k}, \mathbf{k}'}$  represent the coherence factors  $\langle \mathbf{k}' s' | \mathbf{k} s \rangle$  with  $s = s'$  and  $s \neq s'$ , describing the intraband and interband transitions, respectively [26]. The two terms in Eq. (6) describe the processes in which photon absorption is followed by a pair creation, and vice versa. The virtual states in the two contributions, Eq. (6), are characterized by the off-shell energy values  $\varepsilon_{\mathbf{p}} = h\nu + \varepsilon_{\mathbf{k}'_1}$ ,  $\mathbf{p} = \mathbf{k}'_1$  and  $\varepsilon_{\tilde{\mathbf{p}}} = \varepsilon_{\mathbf{k}_1} - h\nu$ ,  $\tilde{\mathbf{p}} = \mathbf{k}_1$  (we use notations from Fig. 2).

As will become clear shortly, the typical energy of secondary pairs  $\omega$  is much smaller than the photon energy  $h\nu$ . Anticipating this result it is convenient to factorize the transition rate, expressing it through the spectral function of

pair excitations. Following the standard route [27], we first split the energy delta function in Eq. (5),

$$\delta_\varepsilon = \int_{-\infty}^{\infty} d\omega \delta(\varepsilon_{\mathbf{k}_1} - \varepsilon_{\mathbf{k}'_1} - h\nu + \omega) \delta(\varepsilon_{\mathbf{k}_2} - \varepsilon_{\mathbf{k}'_2} - \omega).$$

Next, we use the identity  $f_{\mathbf{k}'}(1 - f_{\mathbf{k}}) = (f_{\mathbf{k}'} - f_{\mathbf{k}}) \times (N_{\varepsilon_{\mathbf{k}} - \varepsilon_{\mathbf{k}'}} + 1)$ , where  $N_\omega = 1/(e^{\beta\omega} - 1)$  is the Bose function taken at the electron temperature, and rewrite the sum of  $(f_{\mathbf{k}'_2} - f_{\mathbf{k}_2}) \delta(\varepsilon_{\mathbf{k}_2} - \varepsilon_{\mathbf{k}'_2} - \omega)$  with the help of the relation

$$\text{Im } \Pi(\mathbf{q}, \omega) = -N\pi \sum_{\mathbf{k}_2} \tilde{F}_{\mathbf{k}_2, \mathbf{k}'_2} (f_{\mathbf{k}'_2} - f_{\mathbf{k}_2}) \delta(\varepsilon_{\mathbf{k}_2} - \varepsilon_{\mathbf{k}'_2} - \omega),$$

$\mathbf{q} = \mathbf{k}_2 - \mathbf{k}'_2$ , that follows from the definition of the polarization function [25,28]. This yields a more compact expression for the transition rate:

$$W_{0 \rightarrow 1} = -\frac{2N}{\hbar} \sum_{\mathbf{k}_1, \mathbf{k}'_1, \mathbf{q}, \omega} f_{\mathbf{k}'_1}(1 - f_{\mathbf{k}_1})(N_\omega + 1) |\mathcal{A}'|^2 \text{Im } \Pi(\mathbf{q}, \omega) \times F_{\mathbf{k}_1, \mathbf{k}'_1} |\tilde{V}_{\mathbf{q}, \omega}|^2 \delta_{\mathbf{k}'_1, \mathbf{k}_1 + \mathbf{q}} \delta(\varepsilon_{\mathbf{k}_1} - \varepsilon_{\mathbf{k}'_1} - h\nu + \omega), \quad (7)$$

where  $\omega$  and  $\mathbf{q}$  are the energy and momentum of the soft pair. Here we introduced the quantity

$$\mathcal{A}' = \langle 1 | G(\varepsilon_{\mathbf{p}}, \mathbf{p}) \sigma \mathbf{A} + \sigma \mathbf{A} G(\varepsilon_{\tilde{\mathbf{p}}}, \tilde{\mathbf{p}}) | 1' \rangle, \quad (8)$$

which represents the transition matrix element for the primary (“hard”) pair, factoring out the contribution of the soft pair as described above [we again use a shorthand notation for the electron and hole states  $|\mathbf{k}_1\rangle$  and  $|\mathbf{k}'_1\rangle$  in Fig. 1(c), for brevity suppressing the spin structure].

At this stage it is convenient to approximate the Green’s functions of fermions in the virtual states [ $G(\varepsilon_{\mathbf{p}}, \mathbf{p})$  and  $G(\varepsilon_{\tilde{\mathbf{p}}}, \tilde{\mathbf{p}})$  in Eq. (8)] by expanding in the small frequency  $\omega$  and momentum  $\mathbf{q}$  transferred to the soft pair. This is done by writing  $\varepsilon_{\mathbf{p}} = \varepsilon_{\mathbf{k}_1} + \omega$ ,  $\mathbf{p} = \mathbf{k}_1 + \mathbf{q}$  and  $\varepsilon_{\tilde{\mathbf{p}}} = \varepsilon_{\mathbf{k}'_1} - \omega$ ,  $\tilde{\mathbf{p}} = \mathbf{k}'_1 - \mathbf{q}$  and expanding in  $\omega$  and  $\mathbf{q}$ . The approximation that uses the softness of the secondary pair as a small parameter is known as the “eikonal approximation,” since at small  $\omega$  and  $\mathbf{q}$  only the phase of the fermion wave function varies but not the spinor part. Suppressing the spinor part, we obtain simple expressions

$$G(\varepsilon_{\mathbf{p}}, \mathbf{p}) \approx \frac{-1}{\omega + vq_{\parallel}}, \quad G(\varepsilon_{\tilde{\mathbf{p}}}, \tilde{\mathbf{p}}) \approx \frac{1}{\omega - vq_{\parallel}}, \quad (9)$$

where  $q_{\parallel}$  is the component of  $\mathbf{q}$  parallel to  $\mathbf{k}_1$ . The two terms in (9) originate from the corresponding electron and hole contributions in (8). We note parenthetically that the denominators in Eq. (9) do not vanish since the soft pairs obey  $|\omega| > v|\mathbf{q}|$ . The matrix element  $\mathcal{A}'$  is then reduced to

$$\mathcal{A}' \approx \frac{2vq_{\parallel} \langle 1 | \sigma \mathbf{A} | 1' \rangle}{\omega^2 - v^2 q_{\parallel}^2}. \quad (10)$$

After plugging it in Eq. (7), the quantity  $W_{0 \rightarrow 1}$  becomes

$$W_{0 \rightarrow 1} = -\frac{8N}{\hbar} \sum_{\mathbf{k}_1, \mathbf{q}} |\tilde{V}_{\mathbf{q}, \omega}|^2 \text{Im } \Pi(\mathbf{q}, \omega) \left| \frac{vq_{\parallel} \langle 1 | \sigma \mathbf{A} | 1' \rangle}{\omega^2 - v^2 q_{\parallel}^2} \right|^2, \quad (11)$$



where  $\omega = \hbar\nu - 2v|k_1| - vq_{\parallel}$ . To arrive at Eq. (11) we approximated the intraband coherence factor by unity, since  $F_{k_1, k_1+q} \approx 1$  in the soft-pair limit  $q \ll k_1$ . The interband coherence factor  $F$  has been included in the soft pair spectral function through the factorization procedure outlined above. The factor  $N_{\omega} + 1$ , which we suppressed for brevity, limits summation in Eq. (11) to  $\omega > 0$  for  $T = 0$ . At  $T > 0$ , somewhat counterintuitively, this factor does not impact or regulate the IR divergence (see [12,29] for detailed discussion).

The transition rate  $W_{0 \rightarrow 1}$  features a double-log divergence originating from the collinear  $e$ - $e$  scattering. The divergence arises due singular behavior of the quantities in Eq. (11) upon integration upon the soft-pair momentum  $q$ . In that, one log divergence arises from the integral over the length  $|q|$ , the other log comes from integration over the angle between  $q$  and  $k_1$ . For a quantitative estimate we evaluate the double-log contribution at leading order in  $1/N$ , which can be done by approximating  $\tilde{V}_{q,\omega} \approx -1/\Pi(q, \omega)$ . After integrating over  $q$  and  $k_1$ , and factoring out  $W_{\text{on-shell}}$ , the transition rate for the on-shell diagram in Fig. 1(e), the rate  $W_{0 \rightarrow 1}$  becomes

$$\frac{W_{0 \rightarrow 1}}{W_{\text{on-shell}}} \approx \frac{8}{N\pi^2} \left( \ln \frac{\varepsilon_{>}}{\varepsilon_{<}} \right)^2, \quad W_{\text{on-shell}} = \frac{e^2 A^2 \hbar\nu N}{c^2 8}, \quad (12)$$

where  $\approx$  indicates that contributions subleading to double log were suppressed [12,29]. Here the UV cutoff  $\varepsilon_{>}$  is of order  $\hbar\nu/2$  (energy of an excited electron immediately after photon absorption). The IR cutoff  $\varepsilon_{<}$  is set by the Dirac point width, controlled by carrier collisions or disorder. The  $\log^2$  divergence in Eq. (12) is a direct consequence of linear dispersion, arising from soft secondary pairs that are near-collinear with respect to the primary pair direction and form two counterpropagating jets.

The double-log divergence in the transition rate is reminiscent of the double-log divergences familiar from QCD or QED calculations. This can be seen, e.g., by comparing to soft bremsstrahlung in QED [22], and noting that the double logs arise in an identical manner in both cases, with one log originating from an integral over momentum magnitude and the other from angular integration. As in QED, the IR double-log divergence means that the secondary pairs are much softer than the primary pair, vindicating our eikonal approximation.

The jets formed by soft pairs have random spatial orientation, aligned with the  $e$  and  $h$  velocities of parent hard pairs (see Figs. 1(c)–1(e)). The mean number of pairs in a jet is estimated below. Each jet features a sharp angular distribution that peaks at  $\theta = 0, \pi$  relative to the parent pair direction. The corresponding counting distribution, normalized to the total number of secondary pairs (see [12]), is shown in Fig. 1(e). Energy distribution of soft pairs has a power-law tail at low energies [29].

We parenthetically note that dynamical screening, Eq. (3), is crucial for our analysis. Had an unscreened Coulomb

interaction  $V_q$  been used, the transition rate would have been IR divergent as a power law rather than as  $\log^2$ . This is in line with the argument that the perturbation series for Dirac semimetals should be carried out in powers of a screened interaction rather than the bare one [19]. This behavior is in contrast to QED, where double-log divergences arise from perturbation theory in bare coupling.

Motivated by the resemblance to QED, the higher-order contributions of the form  $N^{-n} \log^{2n}$  can be analyzed by a Sudakov-like resummation scheme of leading double-log divergent diagrams. These diagrams describe primary pair creation followed by emission of multiple secondary pairs in analogy to hard scattering processes in QED accompanied by emission of soft photons. There are soft  $e$ - $h$  pairs of two distinct types emitted, respectively, by the hard electron and the hard hole. These soft pairs form two counterpropagating jets [see Figs. 1(c)–1(e)]. For each of the two jets, in the limit of the emitted pairs being independent of one another and assuming no mutual phase-space blocking, the probability distribution is Poissonian [22],

$$p_n = \frac{\tilde{\lambda}^n}{n!} e^{-\tilde{\lambda}}, \quad \tilde{\lambda} = \frac{4}{N\pi^2} \left( \ln \frac{\varepsilon_{>}}{\varepsilon_{<}} \right)^2. \quad (13)$$

The value  $\tilde{\lambda}$  is a half of the total single-pair emission rate given in Eq. (12). Combining two identical Poisson distributions gives a Poisson counting distribution with a double rate accounting for both jets [12]:

$$\frac{W_{0 \rightarrow n}}{W_{\text{on-shell}}} = \frac{\lambda^n e^{-\lambda}}{n!}, \quad \lambda = 2\tilde{\lambda} = \frac{8}{N\pi^2} \left( \ln \frac{\varepsilon_{>}}{\varepsilon_{<}} \right)^2. \quad (14)$$

The mean number of secondary pairs  $\langle N_{\text{sec}} \rangle = \lambda$  goes as  $\log^2$  and hence can be much greater than unity. As an illustration, a  $\hbar\nu = 1$  eV photon creates between 4 and 10 pairs for ratios  $\varepsilon_{>}/\varepsilon_{<} = 10^2 - 10^3$ , which corresponds to realistic Dirac point widths.

Interestingly, the process in which no soft pairs are emitted has a vanishing rate. Indeed,  $W_{0 \rightarrow 0}$  vanishes in the limit  $\varepsilon_{<} \rightarrow 0$ . To interpret this result we note that the sum of all partial rates equals the bare on-shell rate:  $\sum_{n=0}^{\infty} W_{0 \rightarrow n} = W_{\text{on-shell}}$ . This means that massive emission of soft pairs does not alter the net photon absorption probability. Instead, the absorbed photon energy is redistributed among a large number of secondary  $e$ - $h$  pairs, providing mechanism for carrier multiplication.

In summary, the off-shell pathways unblock kinematic constraints for collinear scattering in a Dirac band, allowing a large number of secondary pairs to be produced as the photogenerated carriers cascade down in energy. The angular distribution of secondary pairs is sharply peaked along the primary pair velocity, representing a condensed-matter analog of relativistic jets familiar from high-energy physics. As discussed above, the jets can be directly probed using a solid-state equivalent of particle detectors [Figs. 1(c), 1(d)]. Formation of jets is corroborated by

recent experimental studies of Auger scattering processes [30,31], which indicate that at weak electron-phonon coupling the collinear scattering processes dominate the relaxation pathways of photoexcited carriers.

We acknowledge support of the Center for Integrated Quantum Materials under NSF Grant No. DMR-1231319, and of MIT Center for Excitonics, an EFRC funded by the U.S. Department of Energy, Office of Science, Basic Energy Sciences under Award No. DE-SC0001088.

- 
- [1] A.H. Castro Neto, F. Guinea, N.M.R. Peres, K.S. Novoselov, and A.K. Geim, *Rev. Mod. Phys.* **81**, 109 (2009).
- [2] J. González, F. Guinea, and M.A.H. Vozmediano, *Phys. Rev. Lett.* **77**, 3589 (1996).
- [3] F. Rana, *Phys. Rev. B* **76**, 155431 (2007).
- [4] M.S. Foster and I.L. Aleiner, *Phys. Rev. B* **79**, 085415 (2009).
- [5] T. Winzer and E. Malić, *Phys. Rev. B* **85**, 241404 (2012).
- [6] D. Brida, A. Tomadin, C. Manzoni, Y. J. Kim, A. Lombardo, S. Milana, R. R. Nair, K. S. Novoselov, A. C. Ferrari, G. Cerullo, and M. Polini, *Nat. Commun.* **4**, 1987 (2013).
- [7] A. Tomadin, D. Brida, G. Cerullo, A. C. Ferrari, and M. Polini, *Phys. Rev. B* **88**, 035430 (2013).
- [8] J. C. W. Song, K. J. Tielrooij, F. H. L. Koppens, and L. S. Levitov, *Phys. Rev. B* **87**, 155429 (2013).
- [9] J. C. W. Song and L. S. Levitov, *J. Phys. Condens. Matter* **27**, 164201 (2015).
- [10] M. Trushin, *Phys. Rev. B* **94**, 205306 (2016).
- [11] M. Schütt, P. M. Ostrovsky, I. V. Gornyi, and A. D. Mirlin, *Phys. Rev. B* **83**, 155441 (2011).
- [12] See Supplemental Material at <http://link.aps.org/supplemental/10.1103/PhysRevLett.120.076601> where additional details are discussed.
- [13] D. Sun, G. Aivazian, A. M. Jones, J. S. Ross, W. Yao, D. Cobden, and X. Xu, *Nat. Nanotechnol.* **7**, 114 (2012).
- [14] M. W. Graham, S.-F. Shi, D. C. Ralph, J. Park, and P. L. McEuen, *Nat. Phys.* **9**, 103 (2013).
- [15] K. J. Tielrooij, M. Massicotte, L. Piatkowski, A. Woessner, Q. Ma, P. Jarillo-Herrero, N. F. van Hulst, and F. H. L. Koppens, *J. Phys. Condens. Matter* **27**, 164207 (2015).
- [16] J. González, F. Guinea, and M. A. H. Vozmediano, *Phys. Rev. B* **59**, R2474 (1999).
- [17] D. T. Son, *Phys. Rev. B* **75**, 235423 (2007).
- [18] E. Barnes, E. H. Hwang, R. E. Throckmorton, and S. Das Sarma, *Phys. Rev. B* **89**, 235431 (2014).
- [19] J. Hofmann, E. Barnes, and S. Das Sarma, *Phys. Rev. Lett.* **113**, 105502 (2014).
- [20] V. N. Gribov and L. N. Lipatov, *Yad. Fiz.* **15**, 781 (1972) [*Sov. J. Nucl. Phys.* **15**, 438 (1972)].
- [21] Y. Dokshitzer, *Basics of Perturbative QCD* (Editions Frontières, Gif-sur-Yvette, France, 1991).
- [22] M. E. Peskin and D. V. Schroeder, *An Introduction to Quantum Field Theory* (Westview Press, Boulder, CO, 1995) Chap. 6.
- [23] R. Jackiw and S. Templeton, *Phys. Rev. D* **23**, 2291 (1981).
- [24] D. Sen, *Phys. Rev. D* **41**, 1227 (1990).
- [25] E. H. Hwang and S. Das Sarma, *Phys. Rev. B* **75**, 205418 (2007).
- [26] T. Ando, *J. Phys. Soc. Jpn.* **75**, 074716 (2006).
- [27] G. F. Giuliani and J. J. Quinn, *Phys. Rev. B* **26**, 4421 (1982).
- [28] B. Wunsch, T. Stauber, F. Sols, and F. Guinea, *New J. Phys.* **8**, 318 (2006).
- [29] C. Lewandowski and L. S. Levitov, [arXiv:1712.06561](https://arxiv.org/abs/1712.06561).
- [30] J. C. König-Otto, M. Mittendorff, T. Winzer, F. Kadi, E. Malic, A. Knorr, C. Berger, W. A. de Heer, A. Pashkin, H. Schneider, M. Helm, and S. Winnerl, *Phys. Rev. Lett.* **117**, 087401 (2016).
- [31] T. Winzer, R. Jago, and E. Malic, *Phys. Rev. B* **94**, 235430 (2016).